Available online at www.sciencedirect.com
ScienceDirect
Earth and Planetary Science Letters 257 (2007) 37–46
EPSL
www.elsevier.com/locate/epsl

# Analysis of waves converted from S to P in the upper mantle beneath the Baltic Shield

Sverker Olsson *, Roland G. Roberts, Reynir Böðvarsson

*Department of Earth Sciences, Uppsala University, Villavägen 16, 75236, Uppsala, Sweden*

Received 25 September 2006; received in revised form 5 February 2007; accepted 6 February 2007
Available online 11 February 2007
Editor: R.D. van der Hilst

**Abstract**

Teleseismic data recorded by broadband stations of the Swedish National Seismic Network have been used in a study of waves converted from S to P in the uppermost mantle. S to P converted waves are recorded as precursors to the direct S arrival. This enables us to study seismic discontinuities at depths of 100–300 km where the traditional receiver function technique based on P to S conversion fails due to disturbances from crustal reverberations. Clear signals of S to P conversion are seen for several horizons in the 50–200 km depth range. This is interpreted as a layered lithosphere with alternating high and low velocity bodies. A sharp contrast is imaged at depths around 160 km and continuous for almost 1000 km in the southern part of the profile. This structure coincides with the velocity contrast interpreted by several authors as the lower limit of a prominent low velocity zone in the 95 to 160 km depth range. A feature which we identify as the lithosphere–asthenosphere boundary is clearly imaged at depths around 200 km.


*Keywords:* lithosphere; asthenosphere; Baltic Shield; converted waves; receiver functions

## 1. Introduction

The FENNOLORA [1] seismic refraction data set collected in 1979 has until recently been the main source of information for detailed seismic investigations of the uppermost mantle of the Swedish part of the Baltic Shield. Recent passive experiments have been focused mainly on other parts of the shield. TOR [2] was designed to probe the Tornquist zone marking the border of the Baltic Shield to the south and SVEKALAPKO [3] studied the Proterozoic–Archean suture in the eastern part of the Shield. In the last few years the number of permanent broadband stations in the Swedish National Seismic Network has grown rapidly, providing an additional teleseismic dataset suitable for the study of the upper mantle.

Analyses of the FENNOLORA data have been carried out using various methods and have shown some disagreement in results [4–9]. What has been agreed upon is the existence of pronounced layering in the lithosphere. Early interpretations of the lower lithosphere include the theses by Guggisberg [4] and Stangl [7]. They both show much layering of the lithosphere, but with fundamentally different characteristics (Fig. 1). Stangl presented a 2-D model with an almost constant lithosphere thickness of 170–175 km

* Corresponding author. Tel.: +46 18 4711475; fax: +46 18 501110.
*E-mail address:* Sverker.Olsson@geo.uu.se (S. Olsson).

0012-821X/$ - see front matter © 2007 Published by Elsevier B.V.
doi:10.1016/j.epsl.2007.02.017

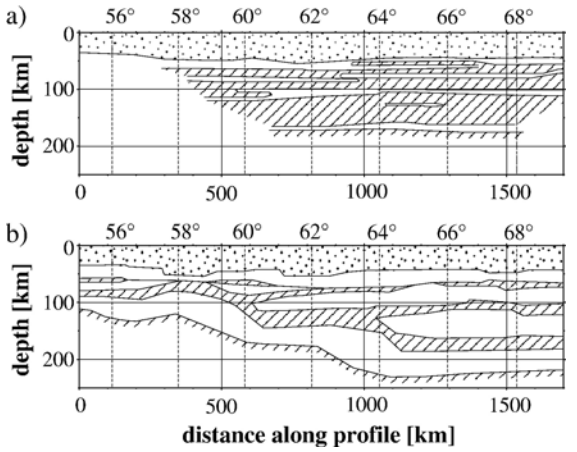


Fig. 1. 2-D models from interpretation of FENNOLORA data. a) Modified from Stangl [7]. b) Modified from Guggisberg [4]. Shaded areas show regions with (relatively) low velocities. The models have been projected on the profile used for analysis in this study (shown in Fig. 2).

and essentially subhorizontal layering of the lithosphere. The interpretation by Guggisberg [4,5] shows significantly more structural heterogeneity. He suggested a lithosphere thickness of more than 200 km in the northern part of the profile but only 110 km for the southernmost part. However, this proposed shallowing of the lithosphere–asthenosphere boundary (LAB) towards the south of Sweden has not been confirmed by other studies. Analyses of data from the TOR experiment [2] all show the Tornquist zone to be a sharp boundary throughout the lithosphere with a lithosphere thickness of at least 200 km for the southernmost part of the Baltic Shield [10,11].

In the interpretation by Stangl, two horizons of increased velocity are modelled at depths fairly constant around 100 km and 160 km throughout the profile. Between these depths, the model contains a broad zone of low velocities. Hauser and Stangl [6] and Stangl [7] also present $Q_P$ models with low values in this depth range. Using FENNOLORA data, Perchuc and Thybo [8] interpret the upper part of the lithosphere (down to 100 km) as a sandwich-layered model of alternating high and low velocity layers. Below this, they propose a zone of low background velocity with isolated high velocity bodies embedded. The low velocity zone (LVZ) bottoms at a depth of 160 km where a continuous high velocity layer is suggested. The existence of a LVZ in this depth range has also been demonstrated by Abramovitz et al. [9] from tomographic inversion of P and S data from the FENNOLORA experiment. This study further showed strong S-wave attenuation below 100 km.

A method well suited to the study of velocity structure at the relevant depths is the analysis of S to P converted waves using teleseismic data. An S wave traversing an impedance contrast may have part of its energy converted to P wave energy. Since the P wave velocity is higher than the S, the converted phase will arrive earlier than the S and may be detected as a precursor to the direct S arrival in the recorded seismogram. This means that signals from the uppermost mantle will not be obscured by signals from crustal reverberations of the main signal, as is the case for the P to S converted waves in the P receiver function technique where reverberations from the Moho or intracrustal structures will cause signals that can effectively mask the signals originating from P to S conversion in the depth range 100–250 km.

In the present study we study precursory signals associated with S to P phase conversion in the upper mantle beneath the Baltic Shield and discuss the observations made in comparison to interpretations from previous studies. We base our analysis on teleseismic data acquired from permanent seismological stations in Sweden.

## 2. Data and processing

SNSN, the Swedish National Seismic Network (Fig. 2) operated by the Department of Earth Sciences at Uppsala University has grown rapidly in the last few years. In 1998, the six stations of the original network were equipped with digital broadband instruments. In 1999–2000, 12 new digital broadband stations were added along the coast of the Gulf of Bothnian. The network was further expanded in 2001–2002, when 20 stations were constructed in the southeast of Sweden along the Baltic coast. In 2003–2004, another set of 7 stations came into operation in the far north of the country. The network is still growing and with the addition of stations in the southwest of Sweden the number of stations will reach 60 at the end of 2006.

The data for this study are 372 seismograms with high quality records of the S arrival. Distances to events used are in the range 67°–95°. This is to ensure that seismograms possess signals from S to P phase conversion in the uppermost mantle. Dominant back azimuths of the dataset are northeast and east (Fig. 2). In the analysis, we have used projection onto the 2-D profile shown in Fig. 2. To restrict the influence of possible three dimensionality on the presented profile, we have excluded data from stations to the west and northwest that are distant from the chosen profile. Stations providing data for this study are given in

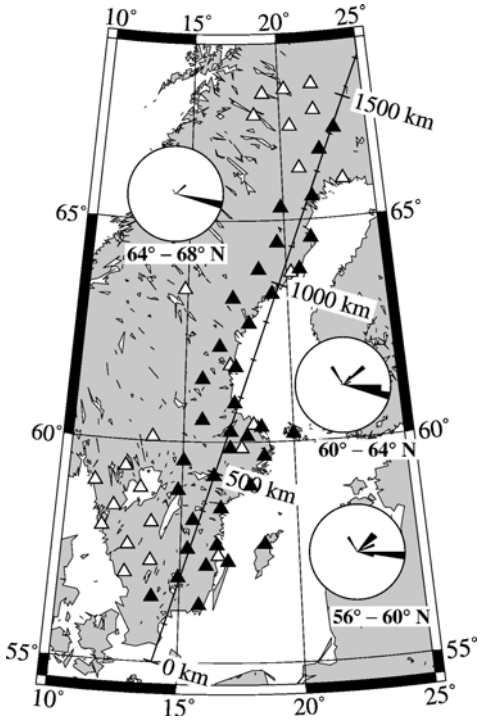


Fig. 2. Map of the study area, showing the location of seismic stations used in this study (solid triangles). Stations not used are shown by open triangles. Circle diagrams show azimuthal distribution of data used sorted to latitude of recording stations. Also shown is the 2-D profile used in the imaging of data.

Table 1. The tectonic evolution of this part of the Baltic shield is thought of as a series of Precambrian orogenies building up to the northeast [12], implying limited structural variation perpendicular to the major axis of the array. Thus, a profile presentation is likely to be well suited to examining the dominant tectonic features.

The method used for analysis is the S receiver function technique [13,14]. In this study we have considered only SV polarized waves converted to P and thus neglected the effects of anisotropy. With this approach we can regard the P component in the time window preceding the direct S arrival as the convolution of the SV component with an S receiver function (SRF), describing the effects of near receiver structures on the incident S wave. To calculate this function we compute the deconvolution of the SV component from the P component. The resulting SRF will be defined at negative time-lags, since S to P converted energy will arrive before the S wave, and will be seen as positive or negative amplitudes in the SRF depending of the polarity of the precursor. For the event distance ranged used in the study of S to P conversion, the incidence angle of the converted P phase will be far from the vertical (30°–40°). The vertical and radial horizontal components therefore need to be rotated to a coordinate system that better separates the P and SV particle motion [14]. Preferably, no S-wave particle motion should be seen on the P component in order to isolate the P converted signal. Several previous applications of the SRF technique rotate components in the vertical plane to minimize amplitudes on the P component at the arrival time of the direct S [14]. In this study, components have been rotated to a coordinate system with minimum cross correlation between P and SV components in a 20 sec time window containing the direct S arrival.

Processing prior to deconvolution includes rotation to the P-SV coordinate system and filtering using a Gaussian shaped lowpass filter, $G(\omega)=\exp(-\omega^2/4a^2)$, where $\omega$ is the angular frequency and the filter width $a=2.0$ was chosen to suppress high frequency noise.

Table 1
SNSN stations providing data for this study

| Station name | Latitude °N | Longitude °E | # SRF |
|---|---|---|---|
| paj | 67.02 | 23.11 | 9 |
| ert | 66.55 | 22.19 | 7 |
| sju | 65.51 | 21.61 | 11 |
| lil | 65.29 | 19.85 | 9 |
| bur | 64.58 | 21.38 | 5 |
| sva | 64.49 | 19.57 | 3 |
| bre | 63.89 | 18.58 | 10 |
| uma | 63.88 | 20.68 | 16 |
| hus | 63.34 | 19.22 | 11 |
| sol | 63.25 | 17.26 | 7 |
| hem | 62.68 | 18.04 | 7 |
| has | 62.15 | 16.61 | 7 |
| arn | 61.69 | 17.38 | 8 |
| rot | 61.42 | 15.81 | 9 |
| igg | 60.87 | 17.32 | 11 |
| fal | 60.49 | 15.83 | 9 |
| gra | 60.33 | 18.54 | 13 |
| ost | 60.23 | 17.13 | 5 |
| aal | 60.18 | 19.99 | 15 |
| fly | 60.13 | 17.88 | 10 |
| bac | 59.85 | 17.11 | 7 |
| nrt | 59.68 | 18.63 | 15 |
| nra | 59.57 | 15.04 | 10 |
| esk | 59.23 | 16.39 | 11 |
| nyn | 59.00 | 18.00 | 12 |
| ask | 58.89 | 14.83 | 12 |
| vik | 58.50 | 16.70 | 14 |
| lnk | 58.22 | 15.50 | 12 |
| got | 57.69 | 18.57 | 17 |
| vst | 57.66 | 16.54 | 16 |
| eks | 57.57 | 15.30 | 13 |
| byx | 57.29 | 17.01 | 9 |
| osk | 57.19 | 16.10 | 11 |
| vxj | 56.92 | 14.94 | 6 |
| del | 56.47 | 13.87 | 13 |
| ble | 56.30 | 15.81 | 11 |

The data are windowed relative to the S arrival predicted by the IASP91 [15] velocity model and good quality data are selected based on a signal to noise criterion (>3.0). Time windows used are −5 to 20 s for the SV component and −40 to 20 s for the P. For deconvolution, the water level source equalization technique of Langston [16] was used.

Several phases have been suggested that may complicate the interpretation of S to P conversions [14,17,18]. Among these are SKS, SKSmp, sPPP and S660sPPP. To eliminate systematic errors introduced by such false precursors, arrival times of these (and similar) phases were calculated for the data using IASP91. Events where "false" precursors were predicted in a time window less than 35 s from direct S were not used for further processing. The strict criteria described above reduced the amount of data suitable for further analysis to 372 seismograms.

S receiver functions calculated from data recorded at the five northernmost stations are shown in Fig. 3a. In the summation trace, the Moho (marked M) is clearly identified as a negative peak at a time of 6–7 s before the S arrival. Other than the Moho, several other possible conversion phases are visible at earlier times. When stacking the SRF, we must however consider the effect of normal moveout due to differences in slowness in the data. For the event distance range used for SRF studies, the difference in arrival time of a phase conversion at 170 km depth may be up to 3 s. In S and P receiver function studies, moveout correction is generally calculated using the IASP91 reference model and the corrected data are often shown relative to the time scale of a reference slowness [14] In this study we have chosen to present the moveout corrected data as depth converted traces as shown in Fig. 3b. At 1 km increments in depth, the advance times of corresponding S to P conversions are calculated using the TauP toolkit [19] and assuming IASP91 velocities. The SRF time series are then resampled as depth series that will align phases that actually originate from phase conversion at a common depth and allow for stacking. In Fig. 3 this is most obvious for a phase (marked L) arriving around 25 s prior to the S. In the depth converted data this phase will stack more coherently to produce a sharper peak in the summation trace at a conversion depth of 200 km.

Fig. 4 shows depth converted SRF for the other stations used in this study. These have been grouped according to station latitude. Within each section, the traces are arranged by the position of their conversion point at 165 km. All sections contain signals that stack coherently in the summation traces. A positive phase marked L certainly corresponds to the phase marked L in Fig. 3. We believe that this phase may be the signal

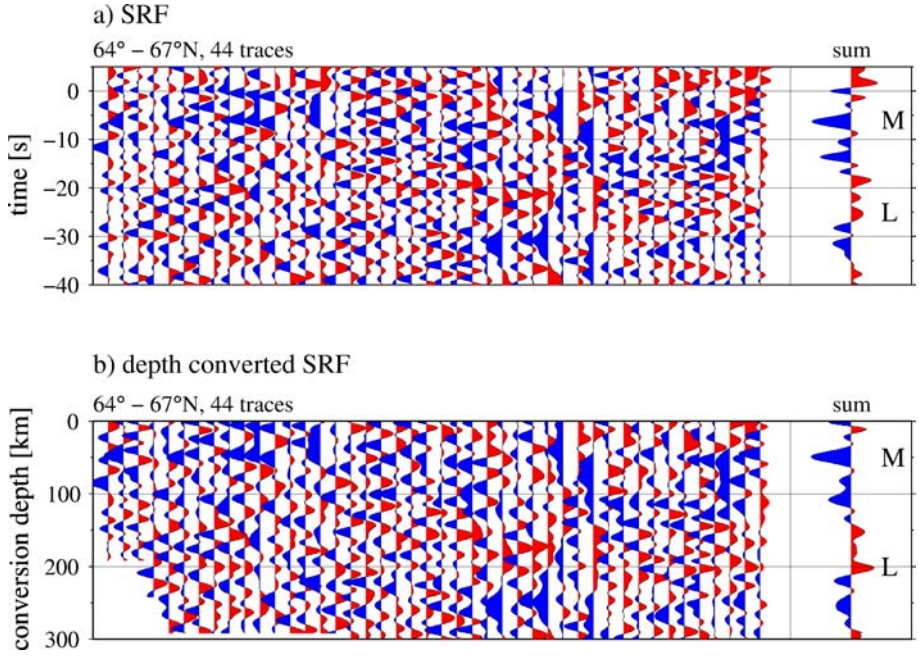


Fig. 3. S receiver functions (SRF) calculated from data recorded at the six northernmost stations. a) Time domain SRF. b) depth converted SRF. Within sections, traces are arranged by epicentral distance. Traces to the right are stacked data. The signal marked L is discussed in the text.

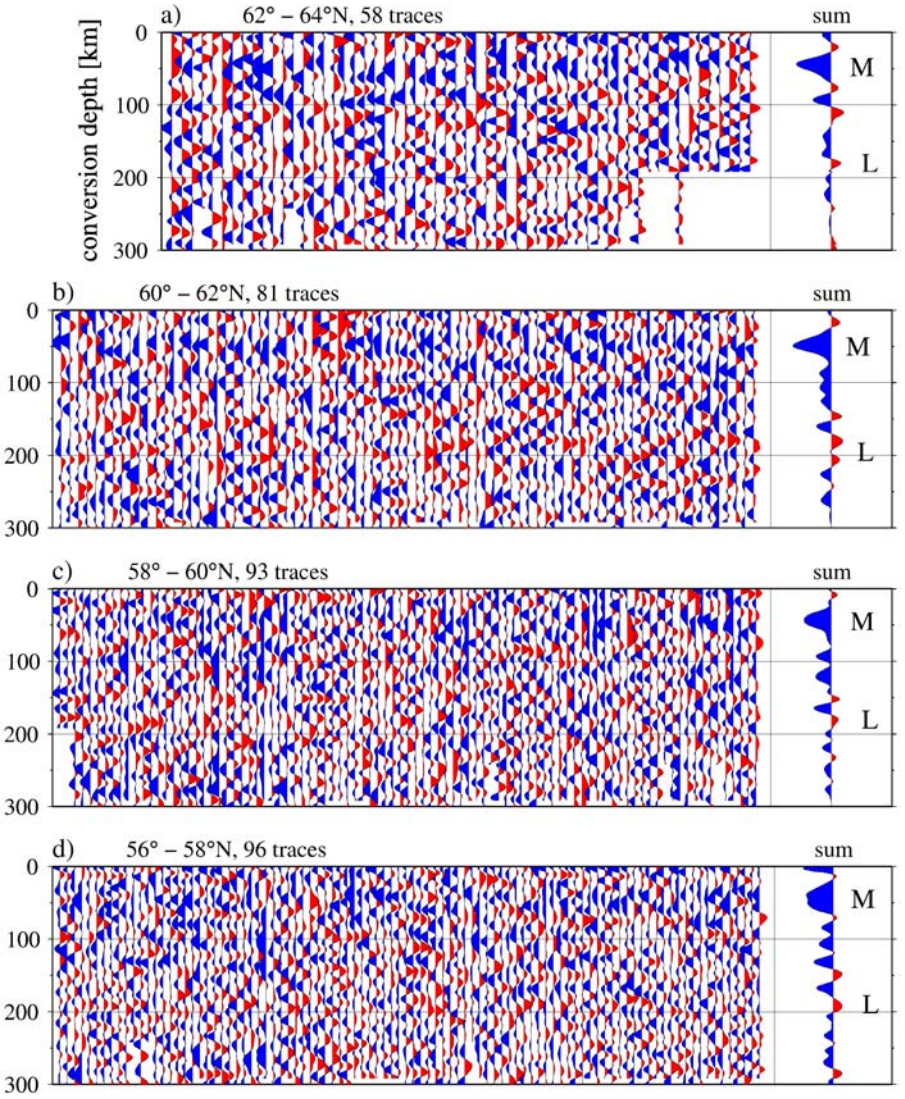


Fig. 4. Depth converted SRF sections. Data have been sorted to station latitude. Within sections, traces are arranged by the projection of a conversion point at 165 km onto the profile shown in Fig. 2. Traces to the right are stacked data. The signal marked L is discussed in the text.

from phase conversion due to a velocity discontinuity at the base of the lithosphere. The phase is weak in Fig. 4c (station latitudes 58°–60°N) and appears to have a doublet in Fig. 4b (60°–62°N). Depth variation of this phase is seen already in a comparison between stacks. There may also be topography of this phase within each section. The very coarse averaging used in Fig. 4 will find horizons that are coherent for hundreds of kilometres, whereas even gently dipping structures may not be visible in the stacked trace. We have therefore chosen to base our interpretation of the data on an alternative imaging technique that considers also the spatial position of conversion points by stacking in a depth migrated spatial domain.

## 3. Imaging

To image upper mantle structures causing S to P conversions, the amplitudes of the SRF are migrated into their spatial position in depth. At 1 km increments in depth, the advance time of corresponding phase conversions and their positions are calculated assuming IASP91 velocities. The depth migrated SRF are then projected onto a 2D-profile along the network and amplitudes are summed in 1 km × 1 km grid cells. The profile is defined by the great circle through points 55°N, 14°E and 67°N, 23°E. Structural variation is imaged by plotting amplitudes using a polar colour scale ranging from blue for negative conversion amplitude to

red for positive amplitudes. Considering particle motions of the direct S wave and the converted P wave implies that negative conversion amplitudes correspond to phase conversions at positive velocity contrasts (velocity increases with depth), whereas positive amplitudes suggest negative velocity contrasts.

The assumption of a IASP91 velocity model will result in errors in the spatial position of depth migrated amplitudes. Tomographic and surface wave studies carried out elsewhere in the Baltic Shield and at the edge of it [10,11,20] suggest higher average upper mantle P and S velocities than in the IASP91 model. To investigate the error bounds of the migration we assume that upper mantle P or S velocities are 5% higher than IASP91 and calculate the wave paths for events at 70°–90°. We then examine the error introduced by migrating using IASP91 velocities. The results of this investigation are presented in Fig. 5. Given that velocity perturbations within this range can be considered reasonable for the study area, the results of Fig. 5 can serve as a guideline for the uncertainty of migrated positions in the resulting image. To accommodate part of the uncertainty introduced by heterogeneities in the overlying velocity structure, we applied spatial averaging in the vertical and horizontal directions using linearly depth dependent averaging windows based on the analysis above (Fig. 5). The halfwidth of the averaging window was taken to be 50% of the conversion depth for the horizontal direction and 10% for the vertical. While this will not correct for systematic errors in depth migration, it will promote coherent stacking of conversion amplitudes in the cases where converted waves have travelled through heterogeneities in overlying velocity structures.

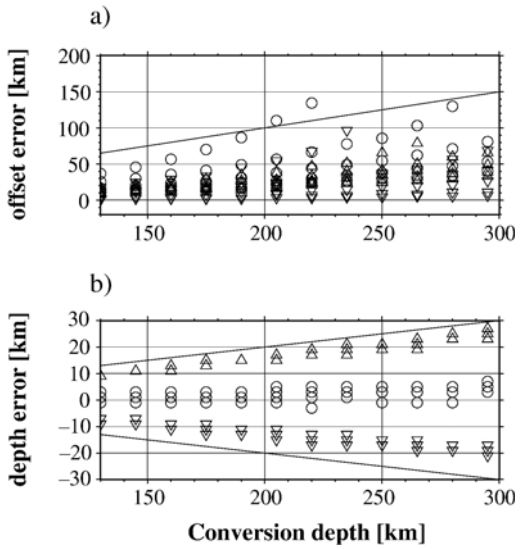


Fig. 5. Analysis of the uncertainty of the lateral position (a) and depth (b) of depth migrated S receiver functions. Advance times of S to P converted waves were calculated for epicentral distances between 70° and 90° for a 5% increase relative to IASP91 in Vs (triangles), Vp (inverted triangles) and both Vs and Vp (circles). Errors in positions are given relative to positions calculated using IASP91 velocities. Dotted lines show halfwidths of the averaging windows applied in horizontal (a) and vertical direction (b).

One other possible cause of error in the depth migration is the effect of crustal thickness variation. This was investigated in a similar fashion by studying the difference in calculated wave paths using uniform one layer crustal models with a thickness between 35 km and 55 km, which is the range of crustal thickness variation expected for the area based primarily on seismic refraction data [4]. It was found that this had a very small effect on migrated positions of deeper conversions and was considered negligible in comparison to the uncertainty introduced by uncertainties in mantle velocities and the scale of the averaging applied.

The resulting image shows several coherent structures along the profile (Fig. 6). First, the Moho is seen from its strong negative amplitudes at depths around 50 km with a variation in depth that is consistent with results from refraction studies [4] and P receiver function analysis. The scatter in the image at Moho depths should probably to large extent be attributed to 3-D heterogeneity in crustal structure not accounted for in this 2-D approximation. Other bands of strong negative amplitudes suggesting a phase conversion from a positive velocity contrast are imaged at depths around 100 km and 160 km (marked A and C in Fig. 6). Positive amplitudes indicating negative velocity contrasts are piecewise coherent at depths 110–120 km (B) and 150 km (D1 and D2). At depths around 200 km, a broad band of positive amplitudes (L) is imaged throughout the profile. North of 65°N we observe a pronounced deepening of several of the imaged features. The onset of this deepening corresponds to the boundary between the Proterozoic and Archean parts of the Baltic Shield [18].

Several of the features observed in the image are geographically very long. Considering the lengths of these and the width of the averaging window at the corresponding depths, this means that data from different sections of the profile will be independent in terms of ray geometry. The horizon of negative amplitude at depth ~160 km is continuous for almost 1000 km. Since averaging in horizontal direction at this depth will distribute SRF amplitudes no more than 160 km along the profile (c.f. Fig. 5), we take this as a

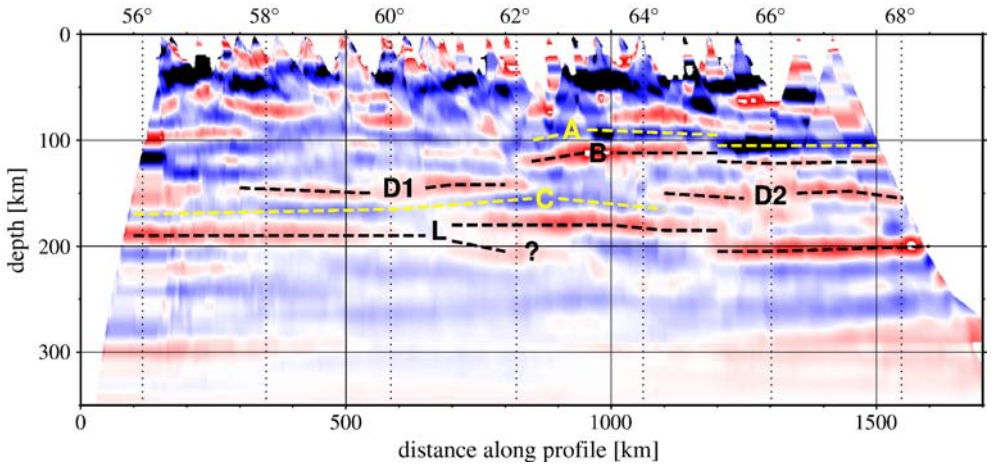


Fig. 6. Resulting image obtained from depth migrated S receiver functions. Negative amplitudes (blue) correspond to S to P conversion from positive (velocity increase with depth) velocity contrasts whereas positive amplitudes (red) suggest negative velocity contrasts. Features of the image that are discussed in the text have been marked in the figure.

strong indication that features of this length scale are reliable.

## 4. Interpretation and discussion

Since the analysis of S to P converted waves is primarily sensitive to large scale horizontal structures, we will discuss our results in comparison to observations from previous studies also sensitive to such features. In Fig. 7 the structural models based on FENNOLORA data and presented in Fig. 1 have been overlaid on the depth migrated SRF image (Fig. 6) to facilitate direct comparison. Although we should not expect to see perfect correlation between images since different velocity models are used, several large scale structures imaged in this study can clearly be correlated to structures also found from the analysis of the FENNOLORA data. A first impression from direct comparison to the FENNOLORA models would certainly be in favor of the interpretation by Stangl (Fig. 1a). The positive velocity contrast imaged at depths around 100 km (marked A in Fig. 6) agrees in depth to the top of the high velocity layer in Stangl's model. In our data, the signal is stronger in the northern part of the profile. Here, signals from a negative velocity contrast (B) can also be detected slightly deeper that might be correlated to the bottom of the high velocity layer in Stangl's model. In the southern part of the profile, these horizons are much weaker and cannot be reliably traced.

The polarity of the horizon imaged at depths around 160 km (C) suggests that it is related to a sharp velocity increase with depth. A similar structure is seen in the results by Stangl. In the interpretation of FENNOLORA data by Perchuc and Thybo [8], a broad zone of low average velocity is suggested at a depth of 95 km in the south and 120 km in the north. Below this a homogeneous high velocity layer is suggested. The signal seen in our data at a depth of 160 km coincides with the velocity contrast interpreted as the base of the suggested LVZ. However, for parts of the profile, our data also shows clear signals from structures within this zone (D1, D2). Even if Perchuc and Thybo [8] see evidence of small scale high velocity bodies within the LVZ, our data clearly suggest that these may exist at scales of hundreds of kilometres. The 2-D model presented by Stangl also contains a high velocity layer embedded within the LVZ between 64° and 66°N. In our data, no internal layering of the LVZ is observed between 62° and 64°N, where our model essentially coincides with the model suggested by Perchuc and Thybo. The top of the proposed LVZ may not be a sharp contrast but a weakly negative gradient, which would explain why it does not show as a continuous horizon of positive SRF amplitudes throughout Fig. 6. A gently dipping structure (B) below 100 km north of 62°N may be associated to the top of this LVZ, but it can not be seen in the southern part of the profile. A horizon of negative amplitudes (A) that may be interpreted as the top of a high velocity lid overlying the LVZ can be traced at depths around 100 km north of 62°N. To the south, this signal is also much weaker. Interestingly, Stangl also models velocity contrasts for the northern segments of FENNOLORA to be sharper than those for the southern part.

The existence of a LVZ in this depth range has been proposed by some workers to be a global characteristic

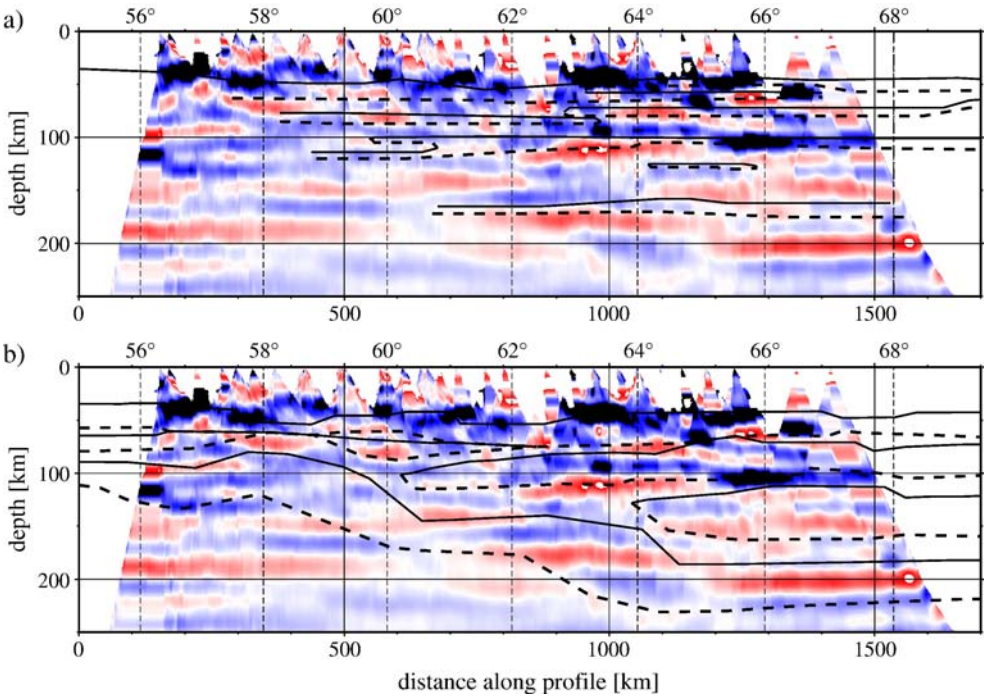


Fig. 7. FENNOLORA models overlaid on the depth migrated SRF image. The lithosphere models suggested by Stangl [7] (a) and Guggisberg [4] (b) have been projected onto the 2-D profile used in the present study and overlaid on the image obtained from depth migration of SRF data. In the FENNOLORA models, solid lines show positive velocity contrasts (velocity increase with depth). Dashed lines are used for negative velocity contrasts.

of continental mantle [21,22]. Such a LVZ could be due to the presence of partial melts. While such a phenomenon might seem less likely below relatively cold shield regions such as the Baltic Shield than below other areas, Thybo and Perchuc [21] argue that small amounts of fluids would lower the solidus curve of a peridotitic mantle enough to produce melts in this depth range for a cold shield geotherm. Using SVEKALAPKO data recorded in the Finnish part of the Baltic Shield, Bruneton et al. [23] also propose this as one possible explanation to their observed discrepancy in the comparison between shear wave velocities derived from surface wave data and velocities derived from compositions of mantle xenolith samples.

The *seismic lithosphere* is generally defined to be an outer shell with higher seismic velocities than the underlying asthenosphere [24]. The LAB in our data would show as a coherent horizon of strong positive amplitude. There is a broad band of positive SRF amplitude at depths around 200 km throughout the profile (L in Fig. 6). We interpret this as the LAB, but the exact continuation of the LAB for parts of the profile is diffuse. The analysis of S to P converted waves is sensitive to velocity contrasts and provides little control of absolute velocities, thus making it difficult to reliably delimit the base of the lithosphere based on this technique alone. As mentioned above, the LAB suggested by Guggisberg [4] does not agree with our data. The model by Stangl [7] suggests a LAB at 170–175 km and thus includes only a thin high velocity layer separating the proposed LVZ and the asthenosphere. Based on P residuals, Babuška et al. [25] report a depth of 180 km for the LAB at ~60°N. These results correlate well to the structure imaged at depths around 190 km for this part of the profile. Results from surface wave studies carried out across the Tornquist zone on the southern edge of the Shield [10], in the eastern part of the shield in Finland [20] and across central parts of the shield [26] all claim a lithosphere thickness of at least 200 km. Thus, assigning the velocity contrast imaged at depths around 200 km as the LAB would be in agreement with previous suggestions on the thickness of the seismic lithosphere.

North of 65°N the LAB appears to deepen below 200 km. This corresponds to the major boundary between the Proterozoic and Archean. The data averaged along the 2-D profile will here consist of contributions from a possibly thicker lithosphere sampled within the Archean core of the Baltic Shield to the northeast [27]. It is also possible that this apparent

deepening of the lithosphere is due to a change in velocities in overlying layers. Resolving this ambiguity between velocity and depth is difficult from analysis of converted phases alone. Recent tomographic results show a sharp contrast from high to low P velocities in the upper 250 km across the Proterozoic–Archean boundary [28]. The relative arrival time of an S to P converted phase is however sensitive to the combination of P and S velocities and results from tomography using S waves are not yet available. Whatever is the complete explanation to the observed deepening of structures across this boundary, our data clearly demonstrates that it is a sharp contrast.

For central parts of the profile (61°–65°N), our data images what appears to be a branching of the LAB. This is in agreement with the results from a previous study of S to P converted phases, where Sacks et al. [17] inferred a lithosphere thickness of 250 km for central parts of the Baltic shield (around 63°N–65°N). We do not however, claim that this structure is reliably determined. Further analysis and a larger amount of high quality data would be required for this and we are therefore at this point not willing to speculate on the nature of this peculiar feature.

Studies of the thickness of the *elastic lithosphere* define the lithosphere as an outer, mechanically elastic shell of the Earth structure. Estimates of this for the Baltic Shield yield values of 70–150 km (see Martinec and Wolf [24] for an account of estimates and methods used). Most recent estimates for the central Baltic shield tend to be close to 100 km [29–31]. This discrepancy between the *seismic* and *elastic* lithosphere thickness is a general observation for shield areas [32]. A thorough investigation on the cause of this ambiguity is obviously beyond the capability of the method used in the present study and beyond the scope of this discussion. It should be noted that our data shows signals from velocity reversals at both suggested LAB depths. In their discussion of the inferred LVZ between 100 and 160 km, Thybo and Perchuc [21] argue that the presence of partial melts in this depth range may lower the viscosity of mantle material [33]. This could explain the lower values of the elastic lithosphere thickness for shield areas obtained by e.g. modelling post-glacial rebound. A more lithosphere-like layer of high velocities underlying this proposed low velocity (and low viscosity) zone would explain the higher values for the thickness of the seismic lithosphere obtained by e.g. surface wave studies. The interpretation of SRF amplitudes in terms of velocity contrasts presented in this study would be in agreement with such a layered model for the upper mantle.

## 5. Summary

The results presented in this study suggest the existence of pronounced layering of the uppermost mantle of the Baltic Shield at depths down to at least 200 km. We base this on the coherent structures seen by S to P conversions, in some cases continuous for up to 1000 km. For the southern part of the profile, a sharp contrast is seen at depths around 160 km with a polarity indicating that velocity increase with depth. This coincides with the velocity contrast interpreted by several authors as the bottom of a low velocity zone. However, our data clearly suggests that this proposed LVZ has internal structure. A clear feature which we identify as the lithosphere–asthenosphere boundary is imaged at depths around 200 km. Deepening of this and other observed features of the profile occurs around 65°N which in this part of the Baltic Shield corresponds to the boundary between Archean and Proterozoic terranes.

Our results support previous interpretations of the lithospheric structure of the Baltic Shield. Furthermore, the image derived by depth migration of S receiver function amplitudes is found to be in agreement with several structures of velocity models independently derived from refraction data. Combined interpretation of results from studies using different methods and independent datasets is essential in any attempt to correctly assess earth structure. We conclude that the study of S to P converted waves serves as a valuable complement to refraction seismic data for the study of the upper mantle.

## Acknowledgements

We thank Hans Thybo and one anonymous reviewer for their valuable comments and suggestions.

## References

[1] C.-E. Lund, Fennoscandian Long-Range Project 1979 (FENNOLORA), Proceedings of the 17th Assembly of the ESC, Budapest, 1980, pp. 511–515.

[2] S. Gregersen, P. Voss, TOR working group, Summary of project TOR: delineation of a stepwise, sharp, deep lithosphere transition across Germany–Denmark–Sweden, Tectonophysics 360 (2002) 61–73.

[3] G. Bock, SVEKALAPKO Seismic Tomography Working Group, Seismic probing of the Fennoscandian lithosphere, Eos, Trans.—Am. Geophys. Union 82 621 (2001) 628–629.

[4] B. Guggisberg, Eine zweidimensionale refraktionsseismiche interpretation der Geschwindligkeits-Tiefen-Struktur des oberen Erdmantels unter dem Fennoskandishen Schild, Diss, ETH Nr 7945, Institute of Geophysics, ETH, Zürich, 1986, 199 pp.

[5] B. Guggisberg, A. Berthelsen, A two-dimensional velocity model for the lithosphere beneath the Baltic Shield and its possible tectonic significance, Terra Cogn. 7 (1987) 631–638.
[6] F. Hauser, R. Stangl, The structure of the crust and the lithosphere in Fennoscandia derrived from a joint interpretation of P- and S-wave data of the FENNOLORA refraction seismic profile, in: R. Freeman, S. Mueller (Eds.), Sixth EGT workshop: Data compilation and synoptic interpretation, European Science Foundation, Strasbourg, 1990, pp. 71–92.
[7] R. Stangl, Die Struktur der Litosphäre in Schweden, abgeleitet aus einer gemeinsamen Interpretation der P- und S-Wellen Registrierungen auf dem FENNOLORA-Profil, Dissertation, University of Karlsruhe, 1990, 187pp.
[8] E. Perchuc, H. Thybo, A new model of upper mantle P-wave velocity below the Baltic Shield: indication of partial melt in the 95 to 160 km depth range, Tectonophysics 253 (1996) 227–245.
[9] T. Abramovitz, H. Thybo, E. Perchuc, Tomographic inversion of seismic P- and S-wave velocities from the Baltic Shield based on FENNOLORA data, Tectonophysics 358 (2002) 151–174.
[10] N. Cotte, H.A. Pedersen, TOR Working group, Sharp contrast in lithospheric structure across the Sorgenfrei–Tornquist zone as inferred by Rayleigh wave analysis of TOR1 project data, Tectonophysics 360 (2002) 75–88.
[11] Z.H. Shomali, R.G. Roberts, Non-linear body wave teleseismic tomography along the TOR array, Geophys. J. Int. 148 (2002) 562–574.
[12] G. Gaal, R. Gorbatschev, An outline of the Precambrian evolution of the Baltic Shield, Precambrian Res. 35 (1987) 15–52.
[13] V. Farra, L. Vinnik, Upper mantle stratification by P and S receiver functions, Geophys. J. Int. 141 (2000) 699–712.
[14] X. Yuan, R. Kind, X. Li, R. Wang, The S receiver functions: synthetics and data example, Geophys. J. Int. 165 (2006) 555–564.
[15] B.L.N. Kennet, E.R. Engdahl, Traveltimes for global earthquake location and phase identification, Geophys. J. Int. 105 (1991) 429–565.
[16] C.A. Langston, Structure under Mount Rainier, Washington, inferred from teleseismic body waves, J. Geophys. Res. 84 (1979) 4749–4762.
[17] I.S. Sacks, J.A. Snoke, E.S. Husebye, Lithosphere thickness beneath the Baltic shield, Tectonophysics 56 (1979) 101–110.
[18] G. Bock, Multiples as precursors to S, SKS and ScS, Geophys. J. Int. 119 (1994) 421–427.
[19] H.P. Crotwell, T.J. Owens, J. Ritsema, The TauP toolkit: flexible seismic traveltime and raypath utilities, Seismol. Res. Lett. 70 (1999) 154–160.
[20] M. Bruneton, V. Farra, H.A. Pedersen, SVEKALAPKO Seismic Tomography Working Group, Non-linear surface wave phase velocity inversion based on ray theory, Geophys. J. Int. 151 (2002) 583–596.
[21] H. Thybo, E. Perchuć, The seismic 8° discontinuity and partial melting in continental mantle, Science 275 (1997) 1626–1629.
[22] H. Thybo, The heterogeneous upper mantle low velocity zone, Tectonophysics 416 (2006) 53–79.
[23] M. Bruneton, H.A. Pedersen, P. Vacher, I.T. Kukkonen, N.T. Arndt, S. Funke, W. Friedrich, V. Farra, SVEKALAPKO Seismic Tomography Working Group, Layered lithospheric mantle in the central Baltic Shield from surface waves and xenolith analysis, Earth Planet. Sci. Lett. 226 (2004) 41–52.
[24] Z. Martinec, D. Wolf, Inverting the Fennoscandian relaxation-time spectrum in terms of an axisymmetric viscosity distribution with a lithospheric root, J. Geodyn. 39 (2005) 143–163.
[25] V. Babuška, J. Plomerová, P. Pajdušak, Seismologically determined deep lithosphere structure in Fennoscandia, GFF Meeting proceedings, Geol. Fören. Stockh. Förh., vol. 110, 1987, pp. 380–382.
[26] G. Calcagnile, Deep structure of Fennoscandia from fundamental and higher mode dispersion of Rayleigh waves, Tectonophysics 195 (1991) 139–149.
[27] S. Sandoval, E. Kissling, J. Ansorge, SVEKALAPKO Seismic Tomography Working Group, High-resolution body wave tomography beneath the SVEKALAPKO array—II. Anomalous upper mantle structure beneath the central Baltic Shield, Geophys. J. Int. 157 (2004) 200–214.
[28] T. Eken, Z.H. Shomali, R.G. Roberts, R. Böðvarsson, Upper mantle structure of the Baltic Shield below the Swedish National Seismic Network (SNSN) resolved by teleseismic tomography, Geophys. J. Int. (in press).
[29] G.A. Milne, J.L. Davis, J.X. Mitrovica, H.-G. Scherneck, J.M. Johansson, M. Vermeer, H. Koivula, Space-geodetic constraints on glacial isostatic adjustment in Fennoscandia, Science 291 (2001) 2381–2385.
[30] G. Kaufmann, K. Lambeck, Glacial isostatic adjustment and the radial viscosity profile from inverse modelling, J. Geophys. Res. 107 (2002) doi:10.1029/2001JB000941.
[31] K. Fleming, Z. Martinec, D. Wolf, A reinterpretation of the Fennoscandian relaxation-time spectrum for a viscoelastic lithosphere, in: I.N. Tziavos (Ed.), Gravity and Geoid, Ziti Publishing, Thessaloniki, Greece, 2003, pp. 432–438.
[32] A.B. Watts, Isostasy and flexure of the lithosphere, Cambridge University Press, Cambridge, 2001.
[33] D.L. Kohlstedt, M.E. Zimmerman, Rheology of partially molten mantle rocks, Annu. Rev. Earth Planet. Sci. 24 (1996) 41–62.